Published in final edited form as:

Clin Cancer Res. 2017 March 15; 23(6): 1481–1492. doi:10.1158/1078-0432.CCR-16-1330.

UNC2025, a MERTK small molecule inhibitor, is therapeutically effective alone and in combination with methotrexate in leukemia models

Deborah DeRyckere[1,2,*], **Alisa B. Lee-Sherick**[3,*], **Madeline G. Huey**[1,2], **Amanda A. Hill**[3], **Jeffrey W. Tyner**[4], **Kristen M. Jacobsen**[1,2,3], **Lauren S. Page**[3], **Gregory G. Kirkpatrick**[3], **Fatma Eryildiz**[5], **Stephanie A. Montgomery**[6,7], **Weihe Zhang**[8], **Xiaodong Wang**[8], **Stephen V. Frye**[7,8], **H. Shelton Earp**[8,9], and **Douglas K. Graham**[1,2]

[1]Aflac Cancer and Blood Disorders Center, Children's Healthcare of Atlanta, Atlanta, GA

[2]Department of Pediatrics, Emory University, Atlanta, GA

[3]Department of Pediatrics, University of Colorado Anschutz Medical Campus, Aurora, CO

[4]Department of Cell, Developmental and Cancer Biology, Oregon Health and Science University, Knight Cancer Institute, Portland, OR

[5]Institute of Environmental Health and Division of Environmental and Biomolecular Systems, Oregon Health and Science University, Portland, OR

[6]Lineberger Comprehensive Cancer Center, University of North Carolina School of Medicine, Chapel Hill, NC

[7]Department of Pathology and Laboratory Medicine, University of North Carolina School of Medicine, Chapel Hill, NC

[8]Center for Integrative Chemical Biology and Drug Discovery, Division of Chemical Biology and Medicinal Chemistry, Eshelman School of Pharmacy, University of North Carolina School of Medicine, Chapel Hill, NC

[9]Departments of Medicine and Pharmacology, University of North Carolina School of Medicine, Chapel Hill, NC

Abstract

Purpose—MERTK tyrosine kinase is ectopically expressed in 30–50% of acute lymphoblastic leukemias (ALL) and over 80% of acute myeloid leukemias (AML) and is a potential therapeutic target. Here, we evaluated the utility of UNC2025, a MERTK tyrosine kinase inhibitor, for treatment of acute leukemia.

Corresponding Author: Douglas K. Graham, MD, PhD, Aflac Cancer and Blood Disorders Center, 4015 Uppergate Dr. Suite 404, Atlanta, GA 30322. Douglas.Graham@choa.org. Phone #404-785-3874, Fax #404-785-1178.

*These authors contributed equally to this work.

Current address for W. Zhang: BioCryst Pharmaceuticals, Inc., 2190 Parkway Lake Drive, Birmingham, AL 35244

Conflict of Interest Disclosures: S.V. Frye, X. Wang, and W. Zhang have filed a patent application describing UNC2025; D.K. Graham, H.S. Earp, S.V. Frye, X. Wang, and D. DeRyckere are stock holders in Meryx, Inc. All other authors report no conflict of interest.

Experimental Design—Pre-clinical *in vitro* and *in vivo* assays using cell lines and primary leukemia patient samples were utilized to evaluate anti-leukemic effect of UNC2025.

Results—UNC2025 potently inhibited pro-survival signaling, induced apoptosis and reduced proliferation and colony formation in MERTK-expressing ALL and AML cell lines and patient samples. Approximately 30% of primary leukemia patient samples (78 of 261 total) were sensitive to UNC2025. Sensitive samples were most prevalent in the AML, T-ALL, and minimally differentiated (M0) AML subsets. UNC2025 inhibited MERTK in bone marrow leukemia cells and had significant therapeutic effects in xenograft models, with dose-dependent decreases in tumor burden and consistent two-fold increases in median survival, irrespective of starting disease burden. In a patient-derived AML xenograft model, treatment with UNC2025 induced disease regression. Additionally, UNC2025 increased sensitivity to methotrexate *in vivo*, suggesting that addition of MERTK-targeted therapy to current cytotoxic regimens may be particularly effective and/or allow for chemotherapy dose reduction.

Conclusions—The broad spectrum activity mediated by UNC2025 in leukemia patient samples and xenograft models, alone or in combination with cytotoxic chemotherapy, support continued development of MERTK inhibitors for treatment of leukemia.

Keywords

MERTK; TAM receptors; small molecule inhibitor; tyrosine kinase inhibitor; chemosensitivity

Introduction

Chemotherapy dose intensification has improved survival in acute leukemia. However those with certain cytogenetic abnormalities or relapsed/refractory disease continue to have a poor prognosis. Additionally, intensive cytotoxic regimens often lead to life-long toxicities (1–4) and are contraindicated in elderly patients due to significant mortality (5, 6). Thus, new approaches are needed.

MERTK is a receptor tyrosine kinase that is ectopically expressed in 30–50% of acute lymphoblastic leukemias (ALL) (7–9) and over 80% of acute myeloid leukemias (AML) (10) and Gas6, a MERTK ligand, has been associated with poor prognosis in AML patients (11). In leukemia cells, MERTK regulates components of downstream signaling pathways that promote tumor cell proliferation and survival, including JAK/STAT, MEK/ERK, p38, PKC, and AKT (7, 9, 10). MERTK transgenic mice develop B- and T-cell leukemias (12) and shRNA-mediated inhibition in ALL and AML cell lines results in delayed leukemogenesis and prolonged survival in orthotopic xenograft models (7, 9, 10). Additionally, inhibition of MERTK sensitizes leukemia cells to cytotoxic chemotherapies (7, 9) and treatment with Gas6 promotes chemoresistance (13), suggesting MERTK inhibition may improve response to chemotherapy and/or allow dose reduction.

While several tyrosine kinase inhibitors (TKIs) have some activity against MERTK, most target other kinases (14). To more potently and selectively inhibit MERTK, we developed UNC2025, an orally-bioavailable small molecule TKI with properties suitable for clinical application (15). UNC2025 inhibits MERTK in enzymatic and cell-based assays, with K_i

and IC_{50} values of 0.16 and 2.7nM, respectively. The compound has similar activity against FLT3 and may be particularly well-suited for treatment of AML where FLT3 is a well-characterized therapeutic target. UNC2025 is selective for MERTK and FLT3, with only 66 of 305 kinases inhibited by >50% at concentrations >100X the MERTK IC_{50} and >45-fold selectivity for MERTK relative to Axl, the next most potently inhibited kinase (K_i = 13.3nM and IC_{50} = 122nM). UNC2025 also has pharmacokinetic properties suitable for *in vivo* studies, including low clearance, a 3.8-hour half-life in mice, 100% oral bioavailability, and high solubility in saline (15). Most importantly, orally-administered UNC2025 inhibits MERTK in bone marrow leukemic blasts for up to 24 hours. Here we describe preclinical studies demonstrating therapeutic effects of UNC2025 in acute leukemia patient samples and animal models supporting further clinical development.

Methods

Cell lines and patient samples

Cell lines were obtained, cultured and identities confirmed as previously described (7, 9, 10). De-identified apheresed patient samples were obtained from University of Colorado after informed consent with approval from the Colorado Multiple Institutional Review Board (IRB) and maintained as previously described (16). De-identified cord blood and normal bone marrow samples were obtained commercially from Clinimmune Labs and ALLCELLS, respectively.

Immunoblot analysis

Leukemia cells ($3x10^6$/mL) were cultured with UNC2025 or DMSO equivalent to 300nM UNC2025 for one hour. Cell lysates were prepared and signaling proteins were detected by immunoblot (antibodies listed in Supplemental Table 1) (15). Cells were treated with pervanadate and MERTK was immunoprecipitated to detect phosphorylated MERTK (15).

Apoptosis, cell cycle, and colony formation assays

Cells were cultured ($3x10^5$/mL) for 6, 24, and/or 48 hours with UNC2025 or DMSO. Apoptotic and dead cells were detected by flow cytometry after staining with YO-PRO-1-iodide and propidium-iodide (7), cell cycle profiles were determined by assessment of propidium iodide staining in permeabilized cells using flow cytometry(17), and MTT reduction was determined as an indicator of viable cell number(17). Alternatively, ALL cell lines and patient samples were cultured in methylcellulose after treatment (10). AML cell lines were cultured in 0.35% Noble agar overlaid with medium containing UNC2025 or vehicle (15). Human mononuclear cells from normal bone marrow or umbilical cord blood were cultured in methylcellulose containing UNC2025 or DMSO (18). Colonies were counted after 7 (normal marrow) or 14 (umbilical cord blood, cell lines and patient samples) days.

Patient sample sensitivity screening

Blood and bone marrow samples were obtained after informed consent with IRB approval at Oregon Health & Science University, Stanford University, University of Utah, UT-Southwestern and University of Colorado-Denver. Mononuclear cells were cultured for 72

hours in 384-well plates with graded concentrations of UNC2025 or vehicle and relative numbers of viable cells were determined (19). IC_{50} values were calculated by non-linear regression.

Leukemia xenograft models

697 cells, monoclonal 697 cells expressing firefly luciferase (20), NOMO-1 cells, or mononuclear cells from an AML patient sample ($2x10^6$/mouse) were injected into the tail vein in NOD.Cg-*Prkdc*^{scid}*Il2rg*^{tm1Wjl}/SzJ (NSG) or NOD.Cg-*Prkdc*^{scid}*Il2rg*^{tm1Wjl}Tg(CMV-IL3,CSF2,KITLG)1Eav/MloySzJ (NSGS) mice. Disease burden was monitored in 697-luciferase xenografts using bioluminescence imaging (21). Peripheral blood, spleen, and bone marrow were collected from patient-derived xenografts and red blood cells (RBCs) were lysed in 50% Dextran sulfate for 15 minutes. Human $CD45^+$ cells were detected using flow cytometry. Mice were distributed to groups with statistically equal disease burden or randomized to groups if leukemia was undetectable. UNC2025 or saline was administered at 10ml/kg once daily by oral gavage. Methotrexate or saline was administered at 5ml/kg by intraperitoneal injection. Mice with advanced leukemia (>20% weight loss, tachypnea, hypothermia, hind-limb paralysis, minimal activity) were euthanized and survival was monitored. Pharmacodynamic studies were performed as previously described (15). Animal experiments were conducted in accordance with regulatory standards as approved by the University of Colorado Institutional Animal Care and Use Committee (Protocol #B-66912(12)1E).

Analysis of hematopoietic precursors and peripheral blood counts

C57Bl/6 mice were treated with UNC2025 or saline daily for 24 days. Peripheral blood was collected into EDTA-coated tubes and complete blood counts were determined using a CBC-Diff Hematology Analyzer (HESKA). Bone marrow cells isolated from leg bones were stained and quantitated using a Gallios flow cytometer (Beckman Coulter) and FlowJo vX software (see Supplemental Table 1) (7).

Statistics

Statistical analyses were performed using GraphPad Prism software (v6.02). Mean values and standard errors are reported. When only two cohorts were compared, data were analyzed using an unpaired t-test. All other data were analyzed using one-way ANOVA with Bonferroni's multiple comparisons correction. Differences were considered significant when $p<0.05$.

Results

UNC2025 inhibits MERTK signaling, induces apoptosis, inhibits proliferation, and decreases colony-formation in MERTK-expressing acute leukemia cell lines

MERTK-expressing B-cell and T-cell acute lymphoid leukemia (B-ALL and T-ALL) and acute myeloid leukemia (AML) cell lines (Figure 1A) were used to determine the effects of UNC2025. Notably, none of the cell lines or patient samples described here have FLT3 activating mutations, therefore observed effects are likely due to MERTK inhibition.

697 B-ALL and Kasumi-1 AML cells were cultured with UNC2025 or vehicle for one hour and phospho-proteins were analyzed. UNC2025 mediated potent and dose-dependent decreases in MERTK phosphorylation/activation in both cell lines (Figure 1B) and inhibition of MERTK correlated with decreased phosphorylation of previously reported MERTK-dependent signaling components STAT6, AKT, and ERK1/2 (Figure 1C).

To investigate functional effects of UNC2025-mediated MERTK inhibition, ALL and AML cell lines were cultured with UNC2025 or vehicle for 48 hours, stained with YO-PRO-1 iodide (YoPro) and propidium iodide (PI) dyes, and analyzed by flow cytometry to identify early apoptotic (YoPro+, PI negative) and late apoptotic or dead (YoPro+, PI+) cells or permeabilized and stained with propidiuim iodide, then analyzed by flow cytometry to determine cell cycle profiles. UNC2025 induced dose-dependent cell death in B-ALL (697, REH), T-ALL (Jurkat), and AML (Kasumi-1, NOMO-1) cell lines (Figure 1D and Supplemental Figures 1A and B). Cell death was induced in 25–90% of cells after 48 hour treatment with 200–300nM UNC2025, corresponding with near complete MERTK inhibition (Figure 1B). Treatment with 200–300nM UNC2025 also altered cell cycle progression with significant decreases in the fraction of cells in G0/G1 phases evident as early as 6 hours post-treatment and more substantial changes after 24–48 hours, including accumulation of cells in G2/M phases (15–94% of cycling cells versus 12–24% in vehicle-treated cultures) and decreased cells in S phase (2–28% of cycling cells versus 21–45% in vehicle-treated cultures) in all 5 cell lines (Figure 1E, Supplemental Figures 1C, E, and F, and Supplemental Table 2). In addition, polyploidy was induced in Jurkat T-ALL and NOMO-1 AML cells. These data demonstrate altered cell cycle progression and are indicative of decreased tumor cell proliferation in response to treatment with UNC2025. Together, decreased tumor cell survival and proliferation led to significantly reduced numbers of viable cells in cultures treated with UNC2025 (Supplemental Figure 1D).

Colony-forming potential was determined to further assess the impact of UNC2025 on oncogenic phenotypes. AML cell lines were cultured in soft agar overlaid with medium containing UNC2025 or vehicle..ALL cell lines were treated with UNC2025 or vehicle for 48 hours and equal numbers of viable cells were cultured in methylcellulose. UNC2025 mediated significant, dose-dependent decreases in colony formation in all cell lines tested with a >50% reduction at 200nM in 3 of 5 cell lines tested in response to treatment with 100nM UNC2025 and near complete abrogation of colony growth in 4 of 5 lines at a dose of 300nM (Figure 1F).

UNC2025 inhibits MERTK signaling and colony-forming potential in a MERTK-expressing patient sample

Similar assays were performed using a MERTK-expressing (AML-123009) primary patient sample. UNC2025 decreased phosphorylation of MERTK and downstream signaling proteins STAT6, AKT, and ERK1/2 (Figures 2A and B). Decreased colony-formation was evident at concentrations as low as 25nM, with >90% inhibition at 300nM (Figure 2C). In contrast, mononuclear cells isolated from normal human cord blood or bone marrow, which express very little or no MERTK (7, 10), were resistant to UNC2025 at doses <500nM (Figure 2D). These data demonstrate selective anti-leukemia effects mediated by UNC2025

in a MERTK-expressing patient sample with a 20-fold difference in sensitivity of MERTK-expressing leukemia blasts relative to normal cord or marrow blood mononuclear cells, suggesting a large therapeutic window.

UNC2025 inhibits expansion of leukemia patient samples in culture

To better characterize effects of UNC2025 in primary samples, expansion of freshly-isolated leukemia cells was assessed using a high-throughput assay. Bone marrow and peripheral blood mononuclear cells from leukemia patients were cultured with UNC2025 or vehicle for 72 hours and the concentration of UNC2025 required to decrease viable cells by 50% (IC_{50}) was calculated. A total of 261 individual samples were analyzed and >60% were collected from patients at first diagnosis. IC_{50} values ranged from 9.0nM to >10μM with a median IC_{50} of 2.38μM (Figure 2E). Sensitivity to UNC2025 was determined relative to the median IC_{50}, with values <475nM (20% of the median) and 238nM (10% of the median) scored as sensitive and very sensitive, respectively. Using this method, 30% of samples (78 of 261) were sensitive and >75% of these (59 of 78) were very sensitive. Sensitive AML, B-ALL, T-ALL, chronic lymphocytic leukemia (CLL), and chronic myeloid leukemia (CML) samples were identified with the greatest percent of sensitive samples in the AML (40%) and T-ALL (50%) subsets. Although the T-ALL subset was small, all four samples tested had IC_{50} values below the median. In the AML subset, sensitivity to UNC2025 was similar in patient samples with and without an activating FLT3 mutation (Supplemental Figure 2). Further subcategorization demonstrated that FAB classification M0 (minimally differentiated) AML samples were consistently particularly sensitive with IC_{50} values <70nM (Figure 2F). In contrast, no myeloproliferative neoplasm (i.e. primary myelofibrosis, systemic mastocytosis, polycthaemia vera, and chronic eosinophilic leukemia) or acute promyelocytic leukemia samples were sensitive to UNC2025. Similarly, although approximately 15% of CML samples were scored as sensitive, the majority (58%) had IC_{50} values >10μM.

UNC2025 inhibits MERTK phosphorylation in bone marrow leukemia cells

Our previous studies demonstrated inhibition of MERTK phosphorylation in bone marrow leukemia cells at T_{max} of 0.5 hours following administration of a single 3mg/kg dose of UNC2025 (15). To determine the dose required to mediate >90% inhibition of MERTK phosphorylation over 24 hours (i.e. the minimum once daily dose to attain continuous MERTK inhibition), 697 B-ALL NSG xenografts were generated and bone marrow cells were collected after a single dose of UNC2025. Lysates were prepared and phosphorylated and total human MERTK levels were determined. After 24 hours, MERTK phosphorylation was significantly decreased by 31% and 66% in 697 cells from mice treated with 3mg/kg or 25mg/kg UNC2025, respectively (Supplemental Figure 3). In contrast, treatment with 75mg/kg sustained robust MERTK inhibition (>90%) over 24 hours. Based on these data, once daily doses of 50mg/kg and 75mg/kg were used for subsequent studies.

UNC2025 mediates minimal and manageable toxicities in mice

To evaluate toxicities associated with UNC2025, C57Bl/6 mice were treated with 75mg/kg UNC2025 for 24 days. Complete blood counts were determined and revealed a significant decrease ($1.46x10^3/\mu L$ versus $5.37\ x10^3/\mu L$) in the total number of white blood cells (WBCs, Figure 3A). Minor alterations in the fractions of lymphocytes and granulocytes

were observed, indicating that all three WBC subsets were similarly affected (Figure 3B). Mice treated with UNC2025 also developed anemia, indicated by significant decreases in RBC number (61%), hemoglobin concentration (61%), and hematocrit (65%) (Figure 3C). The RBCs that were present appeared relatively normal, with significant but minor decreases in cell volume (11%) and distribution width (19%) and a corresponding increase in cellular hemoglobin concentration (11%). There was no significant difference in the number of platelets and a slight but statistically significant increase in platelet volume (7%) (Figure 3D).

To investigate the etiology of these effects, bone marrow progenitor populations were analyzed by flow cytometry. There was a significant 73% decrease in bone marrow cellularity (Figure 3E) with decreased numbers of long-term hematopoietic stem cells (LT-HSCs, 48%), and downstream common myeloid progenitors (CMP, 65%) and megakaryocyte-erythroid progenitors (MEP, 98%) (Figures 3F–G and Supplemental Figure 4). In contrast, there was a statistically significant 96% increase in short-term hematopoietic stem cells (ST-HSCs, Figure 3F). Taken together, the observed increase in the number of ST-HSCs and concomitant reductions in LT-HSCs, more differentiated hematopoietic progenitors, and mature blood cells suggest a developmental arrest at the ST-HSC stage.

Blood electrolytes, indicators of renal function, liver enzymes and albumin concentrations were also analyzed and demonstrated minimal changes, including increased sodium (141mM versus 154mM), decreased blood urea nitrogen (24.2mg/dL versus 18.5mg/dL), and increased alanine transaminase (55.3U/L versus 83.0U/L) (Supplemental Figure 5). Although statistically significant, relative changes of these magnitudes would not require alteration of chemotherapeutic doses in standard leukemia treatment protocols and are unlikely to be clinically relevant. Alkaline phosphatase was more dramatically increased (32.8U/L versus 213.4U/L). The significance of this increase is unknown, but is not usually a dose-limiting laboratory finding in cancer therapeutics. Albumin, a surrogate marker of liver function and malabsorption was not significantly changed.

UNC2025 delays disease progression and prolongs survival in MERTK-dependent orthotopic murine B-ALL and AML xenograft models

NSG mice were inoculated with 697 B-ALL cells expressing the firefly luciferase gene by tail vine injection and treated once daily with 50mg/kg or 75mg/kg UNC2025 or vehicle administered orally. Disease burden was determined by bioluminescence imaging and survival was monitored. In initial studies, treatment began one day after tumor cell inoculation to mimic the disease state after induction therapy. In this model, UNC2025 mediated a statistically significant dose-dependent reduction in tumor burden relative to vehicle (Figures 4A and B). UNC2025 also mediated dose-dependent increases in median survival from 26 days after initiation of treatment in vehicle-treated mice, to 34 and 70 days in mice treated with 50 or 75 mg/kg UNC2025, respectively (Figure 4C). Increases in survival were consistent across multiple experiments (Supplemental Table 3). Interestingly, disease was most evident in the spleen and liver in vehicle-treated mice but was primarily localized to the spinal column and brain in mice treated with UNC2025, suggesting central nervous system involvement (Figure 4A). UNC2025 was penetrant to the brain, but at

reduced concentrations (~25%) relative to plasma (Supplemental Table 4) that are likely too low to mediate significant direct anti-leukemia effects (Figures 4A–C). To test effects of UNC2025 in mice with more substantial disease burden, treatment was delayed until 12 days after leukemia inoculation. Mean pre-treatment disease burden was not significantly different between groups. Disease burden was significantly decreased in mice treated with UNC2025 compared to vehicle (Figure 4D), leading to a two-fold increase in median survival, from 16 to 34 days post-treatment (Figure 4E). In multiple experiments, treatment with UNC2025 consistently increased survival two-fold or greater, even when very high disease burden was present before treatment (Supplemental Table 5). Similar results were observed in NSGS mice with xenografts of the MERTK-dependent NOMO-1 AML cell line. In this case, treatment was initiated 21 days after leukemia inoculation and increased median survival from 15.5 to 37 days post-treatment (Figure 4F). These data demonstrate robust therapeutic activity mediated by UNC2025 *in vivo* in ALL and AML models, irrespective of disease stage.

UNC2025 induces disease regression and prolongs survival in a patient-derived orthotopic murine AML xenograft model

To better recapitulate the biology associated with acute leukemia in humans, an orthotopic patient-derived xenograft model was derived. Primary MERTK-expressing AML blasts were injected intravenously into NSGS mice. Before initiation of treatment there was substantial disease burden in peripheral blood (12.58+/−2.75% blasts), spleen (182+/−48 $x10^6$ blasts) and bone marrow (58.61+/−4.07% blasts) (Figures 5A and B). After 21 days of treatment, disease burden in bone marrow and spleen was not significantly different in vehicle-treated mice compared to the pre-treatment cohort, but peripheral disease was dramatically increased (Figures 5A and B). In contrast, mice treated with 75 mg/kg UNC2025 exhibited significant disease regression in peripheral blood (64%), spleen (50%) and bone marrow (51%) relative to pre-treatment disease burden. In another experiment, peripheral disease burden was monitored throughout the study as an indicator of disease progression and survival was determined. Prior to treatment, there was substantial disease burden in blood (10.61+/−2.15% blasts), bone marrow (39.98+/−7.32% blasts), and spleen (37+/−0.10$x10^6$ blasts). After only three days of treatment, a significant decrease in peripheral disease burden was evident in mice treated with UNC2025 (5.66+/−1.01%; Figure 5C). Additionally, median survival was prolonged from 19.5 to 39 days post-treatment in mice treated with vehicle or UNC2025, respectively (Figure 5D). Nearly identical results were obtained in a repeat experiment (data not shown). Thus, treatment with UNC2025 mediated robust therapeutic activity and was sufficient to induce disease regression and prolong survival in a patient-derived AML xenograft model.

UNC2025 sensitizes 697 ALL cells to treatment with methotrexate in vivo

We previously demonstrated increased sensitivity to cytotoxic chemotherapies in 697 B-ALL cells with shRNA-mediated MERTK inhibition *in vitro*. To determine whether MERTK inhibition has a similar effect *in vivo* and to investigate the potential for application of UNC2025 in the context of current therapeutic regimens, UNC2025 was administered in combination with methotrexate. Mice with orthotopic 697 xenografts were randomized to groups with equal starting disease burden and treated with 75 mg/kg UNC2025 and/or 1

mg/kg methotrexate (Figure 6A). Monotherapy with UNC2025 or methotrexate decreased disease burden relative to vehicle-treated mice, but the combination therapy had a significantly greater effect than either single agent (Figures 6B and C). Similarly, treatment with methotrexate or UNC2025 increased median survival to 61.5 and 72 days after tumor inoculation, respectively, compared to 34 days in vehicle-treated mice and 103.5 days for the combination therapy (Figure 6D). Thus, treatment with single agents was sufficient to prolong survival, but the combination therapy provided a substantially greater benefit. These data demonstrate favorable therapeutic interactions mediated by MERTK inhibition in combination with chemotherapy *in vivo* and indicate that addition of UNC2025 to standard cytotoxic therapies may provide greater therapeutic benefit and/or allow for chemotherapy dose-reduction and decreased toxicity.

Discussion

Previous data demonstrated MERTK over-expression in a spectrum of human cancers, including ALL and AML (14). Additionally, shRNA-mediated MERTK inhibition in acute leukemia cells abrogates oncogenic phenotypes and decreases cell survival, leading to decreased disease burden and prolonged survival in murine xenograft models (7, 9, 10). While these data implicate MERTK as a therapeutic target, they do not distinguish effects of MERTK inhibition on leukemia engraftment versus leukemia progression in animal models. To investigate the therapeutic potential of MERTK inhibition, we developed MERTK-selective TKIs and applied them in animal models. We recently reported prolonged survival mediated by MRX-2843 in MERTK-dependent AML models (22). Here, we describe *in vivo* application of UNC2025, in ALL and AML models in the context of existent disease with a more thorough characterization of impact on disease burden. UNC2025 effectively inhibited phosphorylation of MERTK and its known downstream intracellular targets, induced cell death, decreased colony-forming potential, reduced tumor cell proliferation, and in some cases induced polyploidy *in vitro*. Moreover, UNC2025 inhibited MERTK and had potent therapeutic activity in orthotopic acute leukemia xenograft models. Treatment with UNC2025 delayed disease progression in xenografts of the MERTK-dependent 697 B-ALL cell line and induced disease regression in the bone marrow, spleen and peripheral blood in a primary patient-derived AML xenograft model. Moreover, UNC2025 therapy consistently increased survival two-fold in three different xenograft models, even when extensive disease was present at initiation of treatment. While we cannot rule out the possibility that UNC2025-mediated anti-leukemia activity is enhanced by off-target kinase inhibition, several lines of evidence suggest that this is not the case. First, treatment with UNC2025 recapitulated the effects of shRNA-mediated MERTK inhibition (7, 9, 10). In particular, genetic inhibition of MERTK resulted in dose-dependent increases in median survival in cell line derived orthotopic xenograft models of B-ALL, T-ALL, and AML and efficient MERTK knock-down consistently increased survival two-fold in five different models, including xenografts of the 697 and NOMO-1 cell lines. Additionally, treatment with UNC2025 selectively reduced colony-forming potential in a MERTK-expressing patient sample at concentrations as low as 25nM while mononuclear cells isolated from human cord blood or marrow, which express little or no MERTK, were relatively insensitive to UNC2025, with no effect observed at concentrations ≤500nM. Taken together, these data demonstrate robust

leukemia therapeutic activity mediated by a MERTK-targeted agent with potential for clinical application and provide rationale for further development of UNC2025 or similar MERTK inhibitors for treatment of acute leukemia.

Despite the therapeutic activity mediated by UNC2025 in leukemia models, mice treated with UNC2025 did eventually develop progressive disease, suggesting limited utility for UNC2025 as monotherapy, at least in the absence of the immune system. A better understanding of the mechanisms of resistance to UNC2025 in this context will be important as MERTK inhibitors progress toward clinical development. Possible mechanisms include activation of compensatory signaling pathways, which could be specific to select sites of organ infiltration such as the bone marrow or spleen (e.g. Figure 5). However, even in cases where the leukemia is not sensitive to MERTK inhibition alone, it may be possible to provide enhanced therapeutic activity by combined treatment with a MERTK inhibitor and standard chemotherapeutics or other targeted agents. Indeed, UNC2025 was effective in mice treated with methotrexate, but a combined regimen of UNC2025 and methotrexate mediated more effective inhibition of leukemia progression and a significant increase in median survival relative to either single agent. These data are consistent with previous *in vitro* studies demonstrating increased sensitivity to numerous common cytotoxic chemotherapies, including methotrexate, in acute leukemia cell lines with shRNA-mediated MERTK inhibition (7, 9). We show here that this effect translates to *in vivo* models, suggesting that co-administration of UNC2025 and cytotoxic agents may provide greater benefit and potentially allow chemotherapy dose reduction and decreased long-term side effects. Dose reduction would be particularly advantageous in pediatric and older patient populations.

Although MERTK is expressed in a majority of acute leukemia patient samples, studies investigating the degree of MERTK-dependence in patient samples have not been reported and we do not necessarily expect that all MERTK-expressing samples will be sensitive to MERTK inhibition. Thus, it will be critical to understand the relationship between incidence and requirement for MERTK for effective clinical application of MERTK inhibitors. Here we used a high-throughput assay to characterize the effects of MERTK inhibition on freshly isolated leukemia patient samples. A broad spectrum of sensitivity to UNC2025 was observed, with IC_{50} values ranging from 9nM to >10μM. One-third of samples were sensitive, indicating that a significant fraction of patients could benefit from MERTK inhibition, and sensitive samples were most prevalent in the AML and T-ALL subsets. Of particular interest was the finding that all of the FAB category M0 AML samples were exquisitely sensitive to UNC2025, with IC_{50} values <70nM. Although our analysis of this subset was limited to three samples, these data are encouraging given the incidence (9% of AMLs in adults (23)) and poor prognosis associated with minimally differentiated (M0) AML (24). Similarly, the T-ALL subset was particularly sensitive, with all samples exhibiting IC_{50} values less than the median and half of the samples scored as very sensitive. In contrast, samples with IC_{50} values >10μM were observed in all other subsets. In particular, myeloproliferative neoplasms, acute promyelocytic leukemias and CMLs were relatively resistant to UNC2025. Of note, AML patient samples with and without activating FLT3 mutations were similarly sensitive to UNC2025 and thus, anti-leukemia activity was not solely mediated by FLT3 inhibition in these assays and these data implicate MERTK as a

therapeutic target. Although we did not directly test MERTK expression levels in the samples analyzed here, we and others have previously demonstrated expression of MERTK on >80% of AML patient samples (10, 11). Thus, the observed 40% incidence of UNC2025 sensitivity in AML samples suggests that only a subset of MERTK-expressing samples are dependent on MERTK function and identification of biomarkers and/or assays that can be used in conjunction with MERTK expression to predict response to MERTK inhibitors will be critical for further clinical development.

As development of MERTK inhibitors progresses toward clinical application, it will also be important to anticipate potential side effects. UNC2025 was well-tolerated in mice with minimal and manageable toxicities and was administered daily for up to 110 days with no dose-limiting toxicity, even in combination with methotrexate. The primary side-effects associated with UNC2025 treatment were anemia and leukopenia. Blood count alterations were accompanied by decreased bone marrow cellularity, and reduced numbers of LT-HSCs, CMPs, and MEPs. In contrast, ST-HSCs were increased, suggesting a developmental arrest or delay at this stage leading to decreased generation of more differentiated precursors and mature blood cells. Significant reductions in later stage progenitors have been reported in *Flt3/Flk2* knock-out mice (25, 26) and treatment with AC220, a FLT3 TKI, is associated with pan-leukopenia in mice (27). Anemia and bone marrow suppression have also been noted in clinical trials of FLT3 TKIs (28–30). In contrast, *MERTK* knock-out mice exhibit only a moderate decrease in GMPs with no other defects in hematopoiesis (7, 31). These data suggest that the hematopoietic defects in UNC2025-treated mice are due, at least in part, to FLT3 inhibition. It is encouraging that hematopoietic defects associated with FLT3 inhibition are reversible (27, 28). Notably, accumulation of ST-HSCs in response to treatment with UNC2025 may prime the bone marrow to repopulate the hematopoietic system once therapy is stopped. Alternatively, these cells may have undergone aberrant differentiation to a non-functional ST-HSC phenotype that cannot be further differentiated.

In summary, the studies presented here demonstrate robust therapeutic activity mediated by UNC2025 in cell culture and animal models of acute leukemia. UNC2025 also provided increased therapeutic benefit in combination with methotrexate, suggesting that MERTK inhibition may be a particularly effective therapeutic strategy in the context of cytotoxic chemotherapy, allowing for dose reduction and decreased toxicity. UNC2025 was effective in one-third of freshly isolated leukemia patient samples and our data from a small sample suggest that T-ALL and minimally differentiated AML subsets are particularly sensitive. The incidence of MERTK expression in acute leukemia and the striking and broad spectrum activity mediated by UNC2025 in leukemia patient samples and xenograft models make MERTK a particularly attractive target and the data presented here support further development of UNC2025 or similar inhibitors in early phase clinical trials.

Supplementary Material

Refer to Web version on PubMed Central for supplementary material.

Acknowledgments

Financial support: This work was supported by grants from The Alex's Lemonade Stand Foundation (DKG), the National Cancer Institute (R01CA137078 DKG) (5K12HD068372 ABLS), the American Cancer Society (ACS IRG # 57-001-53 ABLS), and by Federal Funds from the National Cancer Institute, National Institute of Health (Contract No. HHSN261200800001E). J.W.T. is supported by grants from The Leukemia & Lymphoma Society, the V Foundation for Cancer Research, the Gabrielle's Angel Foundation for Cancer Research, and the National Cancer Institute (5R00CA151457-04; 1R01CA183947-01).

This work was supported by grants from The Alex's Lemonade Stand Foundation (DKG), the National Cancer Institute (R01CA137078 DKG) (5K12HD068372 ABLS), the American Cancer Society (ACS IRG # 57-001-53 ABLS), and by Federal Funds from the National Cancer Institute, National Institute of Health (Contract No. HHSN261200800001E). J.W.T. is supported by grants from The Leukemia & Lymphoma Society, the V Foundation for Cancer Research, the Gabrielle's Angel Foundation for Cancer Research, and the National Cancer Institute (5R00CA151457-04; 1R01CA183947-01). The content of this publication does not necessarily reflect the views or policies of the Department of Health and Human Services, nor does mention of trade names, commercial products, or organizations imply endorsement by the U.S. Government. The authors thank the University of Colorado Cancer Center Flow Cytometry Core for technical assistance (NIH P30CA046934), the University of Colorado Diabetes & Endocrinology Research Center Molecular Biology Core Facility (NIH P30DK57516) for cell line authentication services, and the University of North Carolina Mouse Phase 1 Unit (P30 CA016086-40, University Cancer Research Fund) for analysis of blood counts and electrolytes and kidney and liver function tests. Animal histopathology was performed within the LCCC Animal Histopathology Core Facility at the University of North Carolina at Chapel Hill, which is supported in part by NCI Center Core Support Grant (CA16086) to the UNC Lineberger Comprehensive Cancer Center.

References

1. Molgaard-Hansen L, Skou AS, Juul A, Glosli H, Jahnukainen K, Jarfelt M, et al. Pubertal development and fertility in survivors of childhood acute myeloid leukemia treated with chemotherapy only: a NOPHO-AML study. Pediatric blood & cancer. 2013; 60:1988–95. [PubMed: 24038890]
2. Orgel E, Zung L, Ji L, Finklestein J, Feusner J, Freyer DR. Early cardiac outcomes following contemporary treatment for childhood acute myeloid leukemia: a North American perspective. Pediatric blood & cancer. 2013; 60:1528–33. [PubMed: 23441080]
3. Leung W, Hudson MM, Strickland DK, Phipps S, Srivastava DK, Ribeiro RC, et al. Late effects of treatment in survivors of childhood acute myeloid leukemia. Journal of clinical oncology : official journal of the American Society of Clinical Oncology. 2000; 18:3273–9. [PubMed: 10986060]
4. Meadows AT, Friedman DL, Neglia JP, Mertens AC, Donaldson SS, Stovall M, et al. Second neoplasms in survivors of childhood cancer: findings from the Childhood Cancer Survivor Study cohort. Journal of clinical oncology : official journal of the American Society of Clinical Oncology. 2009; 27:2356–62. [PubMed: 19255307]
5. Krug U, Rollig C, Koschmieder A, Heinecke A, Sauerland MC, Schaich M, et al. Complete remission and early death after intensive chemotherapy in patients aged 60 years or older with acute myeloid leukaemia: a web-based application for prediction of outcomes. Lancet. 2010; 376:2000–8. [PubMed: 21131036]
6. Buchner T, Berdel WE, Haferlach C, Haferlach T, Schnittger S, Muller-Tidow C, et al. Age-related risk profile and chemotherapy dose response in acute myeloid leukemia: a study by the German Acute Myeloid Leukemia Cooperative Group. Journal of clinical oncology : official journal of the American Society of Clinical Oncology. 2009; 27:61–9. [PubMed: 19047294]
7. Linger RM, Lee-Sherick AB, Deryckere D, Cohen RA, Jacobsen KM, McGranahan A, et al. Mer receptor tyrosine kinase is a therapeutic target in pre-B cell acute lymphoblastic leukemia. Blood. 2013
8. Graham DK, Salzberg DB, Kurtzberg J, Sather S, Matsushima GK, Keating AK, et al. Ectopic expression of the proto-oncogene Mer in pediatric T-cell acute lymphoblastic leukemia. Clinical cancer research : an official journal of the American Association for Cancer Research. 2006; 12:2662–9. [PubMed: 16675557]

9. Brandao LN, Winges A, Christoph S, Sather S, Migdall-Wilson J, Schlegel J, et al. Inhibition of MerTK increases chemosensitivity and decreases oncogenic potential in T-cell acute lymphoblastic leukemia. Blood Cancer J. 2013; 3:e101. [PubMed: 23353780]
10. Lee-Sherick AB, Eisenman KM, Sather S, McGranahan A, Armistead PM, McGary CS, et al. Aberrant Mer receptor tyrosine kinase expression contributes to leukemogenesis in acute myeloid leukemia. Oncogene. 2013; 32:5359–68. [PubMed: 23474756]
11. Whitman SP, Kohlschmidt J, Maharry K, Volinia S, Mrozek K, Nicolet D, et al. GAS6 expression identifies high-risk adult AML patients: potential implications for therapy. Leukemia. 2014; 28:1252–8. [PubMed: 24326683]
12. Keating AK, Salzberg DB, Sather S, Liang X, Nickoloff S, Anwar A, et al. Lymphoblastic leukemia/lymphoma in mice overexpressing the Mer (MerTK) receptor tyrosine kinase. Oncogene. 2006; 25:6092–100. [PubMed: 16652142]
13. Shiozawa Y, Pedersen EA, Taichman RS. GAS6/Mer axis regulates the homing and survival of the E2A/PBX1-positive B-cell precursor acute lymphoblastic leukemia in the bone marrow niche. Exp Hematol. 2010; 38:132–40. [PubMed: 19922767]
14. Graham DK, DeRyckere D, Davies KD, Earp HS. The TAM family: phosphatidylserine sensing receptor tyrosine kinases gone awry in cancer. Nat Rev Cancer. 2014; 14:769–85. [PubMed: 25568918]
15. Zhang W, DeRyckere D, Hunter D, Liu J, Stashko MA, Minson KA, et al. UNC2025, a potent and orally bioavailable MER/FLT3 dual inhibitor. J Med Chem. 2014; 57:7031–41. [PubMed: 25068800]
16. Klco JM, Spencer DH, Lamprecht TL, Sarkaria SM, Wylie T, Magrini V, et al. Genomic impact of transient low-dose decitabine treatment on primary AML cells. Blood. 2013; 121:1633–43. [PubMed: 23297133]
17. Macy ME, DeRyckere D, Gore L. Vandetanib mediates anti-leukemia activity by multiple mechanisms and interacts synergistically with DNA damaging agents. Invest New Drugs. 2012; 30:468–79. [PubMed: 21046425]
18. Lee-Sherick AB, Zhang W, Menachof KK, Hill AA, Rinella S, Kirkpatrick G, et al. Efficacy of a Mer and Flt3 tyrosine kinase small molecule inhibitor, UNC1666, in acute myeloid leukemia. Oncotarget. 2015; 6:6722–36. [PubMed: 25762638]
19. Tyner JW, Yang WF, Bankhead A 3rd, Fan G, Fletcher LB, Bryant J, et al. Kinase pathway dependence in primary human leukemias determined by rapid inhibitor screening. Cancer research. 2013; 73:285–96. [PubMed: 23087056]
20. Christoph S, Schlegel J, Alvarez-Calderon F, Kim YM, Brandao LN, DeRyckere D, et al. Bioluminescence imaging of leukemia cell lines in vitro and in mouse xenografts: effects of monoclonal and polyclonal cell populations on intensity and kinetics of photon emission. J Hematol Oncol. 2013; 6:10. [PubMed: 23343252]
21. Christoph S, Lee-Sherick AB, Sather S, DeRyckere D, Graham DK. Pre-clinical evaluation of tyrosine kinase inhibitors for treatment of acute leukemia. J Vis Exp. 2013:e50720. [PubMed: 24084362]
22. Minson KA, Smith CC, DeRyckere D, Libbrecht C, Lee-Sherick AB, Huey MG, et al. The MERTK/FLT3 inhibitor MRX-2843 overcomes resistance-conferring FLT3 mutations in acute myeloid leukemia. JCI Insight. :1.
23. Venditti A, Del Poeta G, Buccisano F, Tamburini A, Cox MC, Stasi R, et al. Minimally differentiated acute myeloid leukemia (AML-M0): comparison of 25 cases with other French-American-British subtypes. Blood. 1997; 89:621–9. [PubMed: 9002966]
24. Barbaric D, Alonzo TA, Gerbing RB, Meshinchi S, Heerema NA, Barnard DR, et al. Minimally differentiated acute myeloid leukemia (FAB AML-M0) is associated with an adverse outcome in children: a report from the Children's Oncology Group, studies CCG-2891 and CCG-2961. Blood. 2007; 109:2314–21. [PubMed: 17158236]
25. McKenna HJ, Stocking KL, Miller RE, Brasel K, De Smedt T, Maraskovsky E, et al. Mice lacking flt3 ligand have deficient hematopoiesis affecting hematopoietic progenitor cells, dendritic cells, and natural killer cells. Blood. 2000; 95:3489–97. [PubMed: 10828034]

26. Mackarehtschian K, Hardin JD, Moore KA, Boast S, Goff SP, Lemischka IR. Targeted disruption of the flk2/flt3 gene leads to deficiencies in primitive hematopoietic progenitors. Immunity. 1995; 3:147–61. [PubMed: 7621074]

27. Taylor SJ, Dagger SA, Thien CB, Wikstrom ME, Langdon WY. Flt3 inhibitor AC220 is a potent therapy in a mouse model of myeloproliferative disease driven by enhanced wild-type Flt3 signaling. Blood. 2012; 120:4049–57. [PubMed: 22990016]

28. Knapper S, Burnett AK, Littlewood T, Kell WJ, Agrawal S, Chopra R, et al. A phase 2 trial of the FLT3 inhibitor lestaurtinib (CEP701) as first-line treatment for older patients with acute myeloid leukemia not considered fit for intensive chemotherapy. Blood. 2006; 108:3262–70. [PubMed: 16857985]

29. Cortes JE, Kantarjian H, Foran JM, Ghirdaladze D, Zodelava M, Borthakur G, et al. Phase I study of quizartinib administered daily to patients with relapsed or refractory acute myeloid leukemia irrespective of FMS-like tyrosine kinase 3-internal tandem duplication status. Journal of clinical oncology : official journal of the American Society of Clinical Oncology. 2013; 31:3681–7. [PubMed: 24002496]

30. Chen YB, Li S, Lane AA, Connolly C, Del Rio C, Valles B, et al. Phase I trial of maintenance sorafenib after allogeneic hematopoietic stem cell transplantation for fms-like tyrosine kinase 3 internal tandem duplication acute myeloid leukemia. Biol Blood Marrow Transplant. 2014; 20:2042–8. [PubMed: 25239228]

31. Wang H, Chen S, Chen Y, Wang H, Wu H, Tang H, et al. The role of Tyro 3 subfamily receptors in the regulation of hemostasis and megakaryocytopoiesis. Haematologica. 2007; 92:643–50. [PubMed: 17488688]

Statement of Clinical Relevance

This manuscript describes characterization of UNC2025, a novel MERTK tyrosine kinase inhibitor, for potential use in the treatment of acute lymphoblastic and acute myeloid leukemias (ALL and AML, respectively). Our previous data validate MERTK as an oncogenic target and demonstrate roles for MERTK in chemo-resistance. Here we advance these findings using UNC2025, a novel orally bioavailable MERTK-targeted small molecule inhibitor. Treatment with UNC2025 induced apoptosis and decreased clonal proliferation in acute leukemia cell lines and patient samples *in vitro* and prolonged leukemia-free survival and sensitivity to cytotoxic chemotherapy in cell line and patient-derived xenograft models. Of note, 30% of freshly isolated patient samples were sensitive to UNC2025 suggesting that a large fraction of patients with acute leukemia could benefit from MERTK-targeted therapy. These data support continued development of MERTK small molecule inhibitors toward clinical application in patients with ALL and AML.

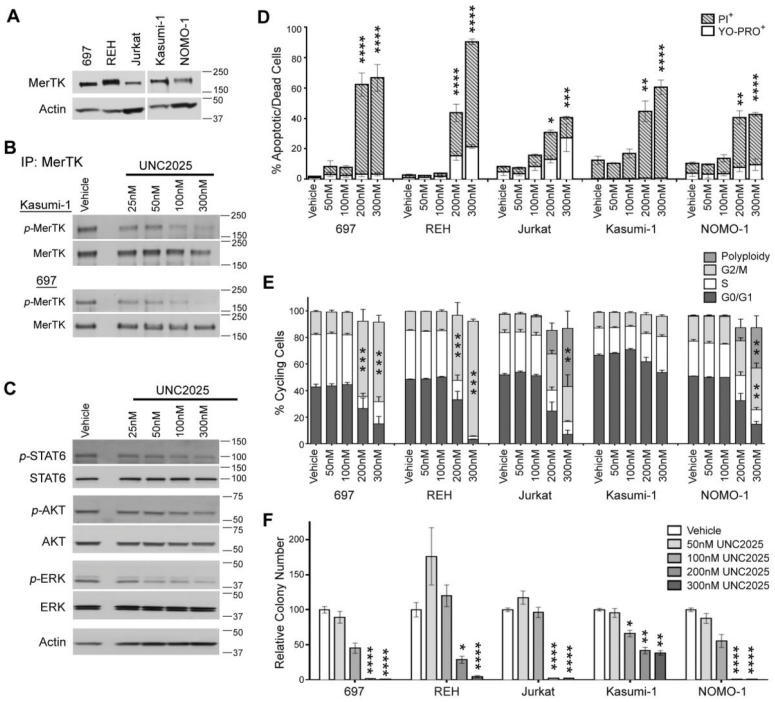

Figure 1. UNC2025 inhibits *p*-MERTK and downstream signaling, induces apoptosis,inhibits proliferation and colony formation, and induces polyploidy in acute leukemia cell lines

(**A**) MERTK expression (~180 kDa) in the indicated cell lines was assessed by immunoblot. (**B**) Kasumi-1 AML (top panels) and 697 B-ALL (lower panels) cells were treated with vehicle (DMSO) or the indicated dose of UNC2025 for one hour and pervanadate phosphatase inhibitor was added to the cultures for three minutes to stabilize phosphorylated proteins. MERTK was immunoprecipitated from cell lysates and phosphorylated (denoted with *p*-) and total MERTK proteins were detected by immunoblot. (**C**) Kasumi-1 cells were treated with DMSO or the indicated dose of UNC2025 for one hour and phosphorylated and total STAT6, AKT and ERK1/2 downstream signaling proteins were detected by immunoblot. Actin is shown as a loading control. (**D–E**) B-ALL (697, REH), T-ALL (Jurkat), and AML (Kasumi-1, NOMO-1) cell lines were treated with the indicated concentration of UNC2025 or DMSO for 48hours, then stained with YO-PRO-1 iodide and propidium iodide and analyzed by flow cytometry. Alternatively, cells were fixed, permeabilized and cell cycle profiles as indicated by DNA content were determined by flow cytometry. (**D**) Percentages of early apoptotic and late apoptotic/dead cells are shown. Mean values and standard errors were derived from 3–7 independent experiments. **(E)** Percentages of cycling cells in G0/G1, S, and G2/M phases and cells with >4N DNA content (Polyploid) are shown. Mean values and standard errors were derived from 3 independent experiments. Statistically significant differences in the fractions of cells in G2/M phase or with a polyploid phenotype are indicated. Additional statistical data are included in Supplemental Table 1. (**F**) ALL cell lines (697, REH, Jurkat) were cultured in liquid medium with the indicated concentration of UNC2025 or DMSO for 48 hours and then equal numbers of viable cells were cultured in methylcellulose medium in the absence of UNC2025. Alternatively, AML cell lines (Kasumi-1, NOMO-1) were cultured in soft agar overlaid with

medium containing vehicle or the indicated concentration of UNC2025, without prior drug pre-treatment. Colonies were stained with MTT reagent after 10–21 days and counted. Colony numbers relative to vehicle-treated cultures are shown. Mean values and standard errors were derived from 3 independent experiments. (*p<0.05, **p<0.01, ***p< 0.001, ****p< 0.0001, 1-way ANOVA)

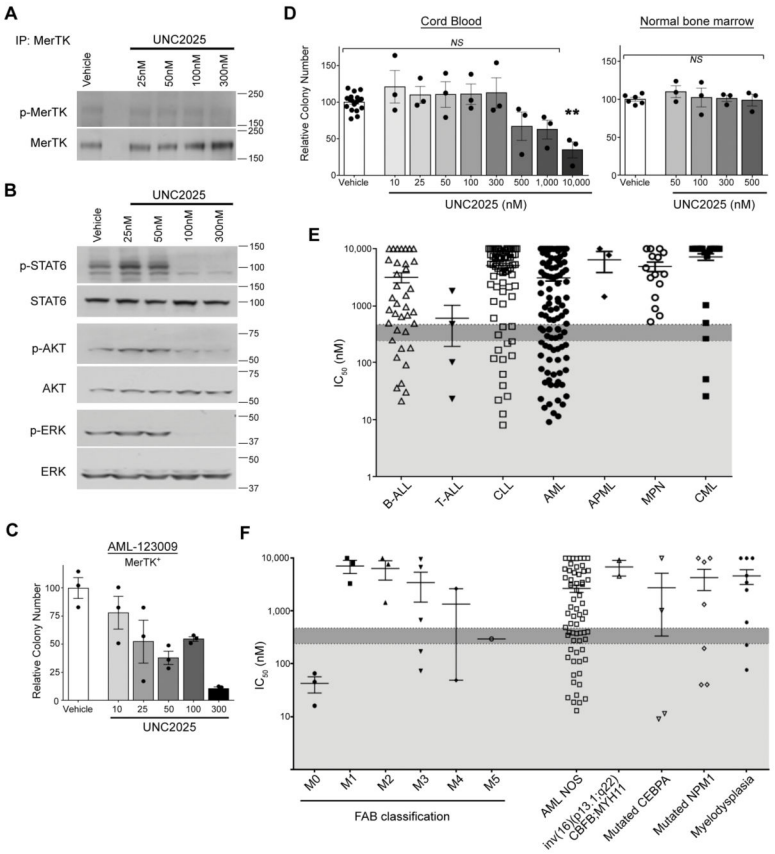

Figure 2. UNC2025 inhibits *p*-MERTK and downstream signaling and inhibits expansion of leukemia patient samples in culture

(**A**) Mononuclear cells isolated from primary AML patient sample AML-123009 were treated with vehicle (DMSO) or the indicated dose of UNC2025 for one hour and phosphorylated (denoted by *p*-) and total MERTK proteins were assessed as described in Figure 1. (**B**) Downstream signaling was assessed in the AML-123009 patient sample after one hour treatment with vehicle or UNC2025 as described in Figure 1. (**C**) Mononuclear cells isolated from the MERTK-expressing AML-123009 patient sample was treated with vehicle or UNC2025 for 48 hours and then cultured in methylcellulose as described in Figure 1. Colony numbers relative to vehicle-treated cultures are shown. Mean values and standard errors were derived from triplicate samples from a single experiment. (**D**) Umbilical cord blood and bone marrow mononuclear cells collected from 3 different healthy donors were cultured in methylcellulose medium containing vehicle or UNC2025 for 7–14 days. Colonies were stained and counted as in Figure 1. Colony numbers relative to vehicle-treated cultures are shown. Mean values and standard errors were derived from three independent experiments (**$p<0.01$, *NS* = not significant, 1-way ANOVA). (**E–F**) Mononuclear cells isolated from primary bone marrow or peripheral blood samples collected from patients with hematologic malignancies were cultured in 384-well plates in liquid media containing vehicle or UNC2025 (14nM–10μM) for 72 hours and reduction of MTS tetrazolium was determined as an indicator of viable cell number. Half maximal inhibitory concentrations (IC_{50}) were determined by non-linear regression. IC_{50} values less than

0.24μM (indicated by light grey shading) and 0.475μM (indicated by dark grey shading) were scored as very sensitive and moderately sensitive, respectively. (**E**) Patient samples are shown grouped by hematologic malignancy subtype. (**F**) AML patient samples are shown grouped by French-American-British (FAB) classification on the left side of the graph and by molecular lesion on the right.

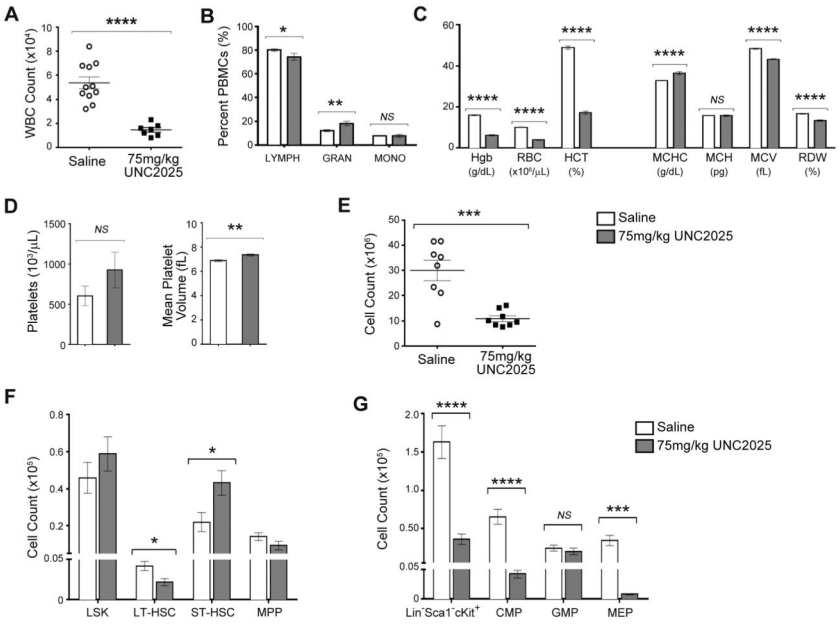

Figure 3. Treatment with UNC2025 alters bone marrow progenitor populations and decreases white and red blood cell numbers

C57Bl/6 mice were treated with 75mg/kg UNC2025 (gray bars) or an equivalent volume of saline (white bars) once daily for 24 days. Bone marrow and peripheral blood were harvested. Complete blood counts were determined and bone marrow progenitor populations were analyzed by flow cytometry. (**A**) Peripheral white blood cell (WBC) counts. (**B**) Percentages of lymphocytes, granulocytes and monocytes in peripheral blood mononuclear cells. (**C**) Red blood cell counts and indices. (**D**) Platelet counts and volumes. (**E**) Number of nucleated cells in the bone marrow. (**F**) Numbers of stem cells and multi-potent progenitor cells. (**G**) Numbers of Lin^- $Sca1^-$ $cKit^+$ and myeloid progenitor cells. Mean values and standard errors are shown (n=7 or 11). (*p<0.05, **p<0.01, ***p<0.001, ****p<0.0001, *NS* = not significant, unpaired t-test)

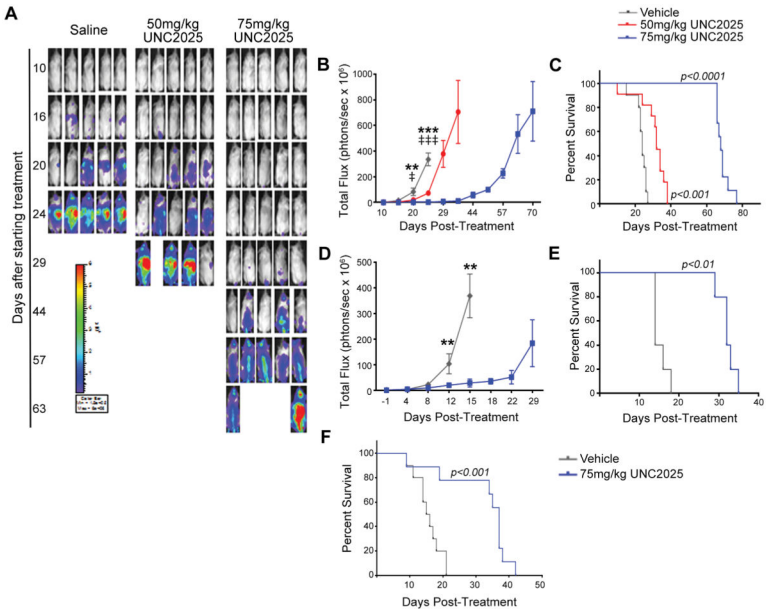

Figure 4. UNC2025 delays disease progression and prolongs survival in MERTK-dependent orthotopic ALL and AML xenograft models

(**A–E**) 697 B-ALL cells expressing the firefly luciferase gene were inoculated into NOD-SCID-gamma (NSG) mice by tail vein injection. Mice were treated once daily with 50 or 75 mg/kg UNC2025 or an equivalent volume of saline beginning one day after tumor cell inoculation (A–C) to model minimal residual disease (MRD) or 12 days after tumor cell inoculation (D–E) to model existent disease. Disease burden was determined by bioluminescence imaging and survival was monitored. (**A**) Representative bioluminescent images of the 697 MRD model. (**B**) Bioluminescence intensity over time in the 697 MRD model. (n=9–11, ** p<0.01, **** p<0.0001, ‡ p<0.05, ‡‡‡‡ p<0.0001, 1-way ANOVA; * denotes comparison between saline and 75mg/kg UNC2025, ‡ denotes comparison between saline and 50mg/kg UNC2025). (**C**) Kaplan-Meier curves derived from the 697 MRD model. Median survival was 26, 34, and 70 days after initiation of treatment in mice treated with vehicle, 50mg/kg UNC2025, and 75mg/kg UNC2025, respectively (n = 9–11; log rank test). (**D**) Bioluminescence intensity over time in the 697 existent disease model. (n=5, ** p<0.01 compared to saline, 1-way ANOVA). (**E**) Kaplan-Meier curves derived from the 697 existent disease model. Median survival was 16 and 34 days after initiation of treatment in mice treated with vehicle and 75mg/kg UNC2025, respectively (n = 5; log rank test). (**F**) NOMO-1 AML cells were inoculated into NSG mice expressing human cytokines (NSGS) by tail vein injection. Mice were treated once daily with UNC2025 or an equivalent volume of saline beginning 21 days after tumor cell inoculation and survival was monitored. Kaplan-Meier curves are shown demonstrating median survival of 15.5 and 37 days after initiation of treatment with vehicle and 75mg/kg UNC2025, respectively (n = 9–10; log rank test).

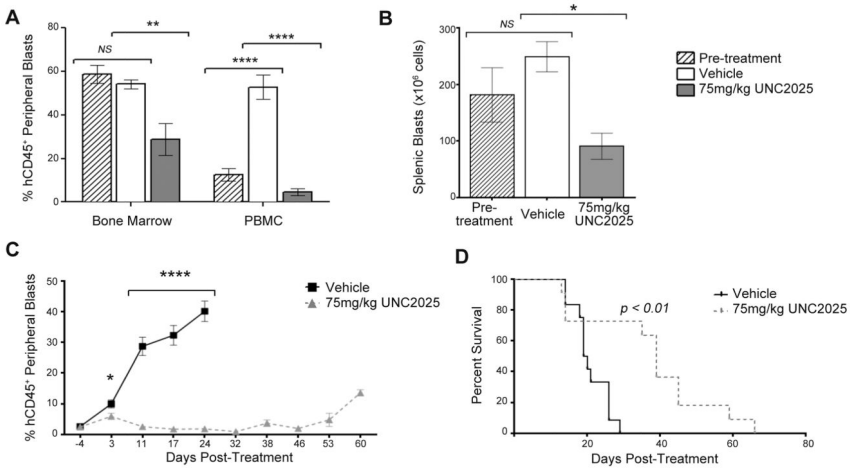

Figure 5. UNC2025 induces disease regression and prolongs survival in an orthotopic patient-derived AML xenograft model

NSGS mice were inoculated with mononuclear cells isolated from the MERTK-expressing AML-123009 primary patient sample. Once daily treatment with 75mg/kg UNC2025 or an equivalent volume of saline vehicle was initiated 41 days after tumor cell inoculation. Peripheral blood, bone marrow, and spleen were harvested and leukemic blasts (human CD45+) were detected by flow cytometry. Survival was monitored. (**A**) Percentages of leukemic blasts in bone marrow and peripheral blood before initiation of treatment, and 21 days after initiation of treatment (n=6–7; 1-way ANOVA). (**B**) Numbers of blasts in the spleen before treatment and after 21 days of treatment (n=6–7; 1-way ANOVA). (**C**) Percent blasts in peripheral blood over time (n = 11–12; unpaired t-test). (**D**) Kaplan-Meier curves demonstrating median survival of 19.5 and 39 days after initiation of treatment with saline or UNC2025, respectively (n=11–12; log-rank test). (*p< 0.05, **p < 0.01, ****p < 0.0001, NS = not significant).

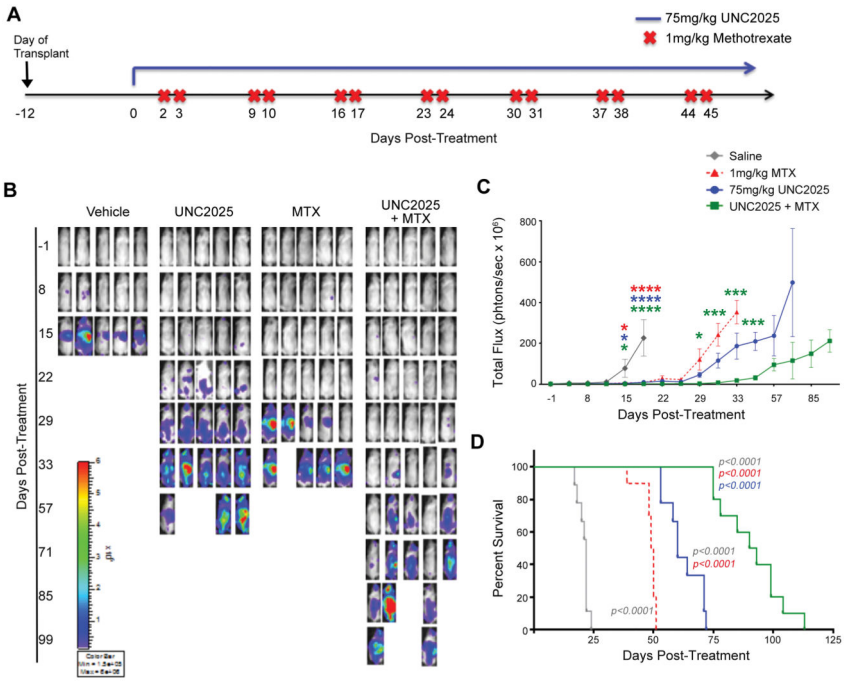

Figure 6. UNC2025 provides additional therapeutic benefit in combination with methotrexate *in vivo*

697 B-ALL xenografts were generated in NSG mice as described in Figure 4. (**A**) Schematic of treatment administration. Once daily treatment with 75mg/kg UNC2025 or an equivalent volume of saline was initiated 12 days after tumor cell inoculation. 1mg/kg methotrexate (MTX) or an equivalent volume of vehicle (DMSO) was administered on two consecutive days per week for six weeks beginning 14 days after tumor inoculation. (**B**) Representative bioluminescent images are shown. (**C**) Bioluminescence intensity over time (n=10, *p<0.05, ***p<0.001, ****p<0.0001, 1-way ANOVA; red asterisks denote comparison between saline and methotrexate, blue asterisks denote comparison between saline and UNC2025 monotherapy, green asterisks denote comparison between the indicated treatment and combination therapy) (**D**) Kaplan-Meier curves are shown demonstrating median survival of 34 days after initiation of treatment with vehicle, 61.5 days for MTX, 72 days for 75 mg/kg UNC2025, and 103.5 days for combination therapy (n = 10). Statistical comparisons versus saline are shown in gray, versus methotrexate in red, and versus UNC2025 in blue (log rank test).